Photochemistry and Photobiology, 1996, 64(3): 407–418

Symposium-in-Print

Spectral Modeling of UV Inhibition of *In Situ* Antarctic Primary Production Using A Field-Derived Biological Weighting Function

Nicolas P. Boucher[1] and Barbara B. Prézelin*[2]

[1]Laboratoire d'Ecologie Marine, Université de La Réunion, La Réunion, France and
[2]Department of Ecology, Evolution and Marine Biology and Center for Remote Sensing and Environmental Optics, University of California, Santa Barbara, Santa Barbara, CA, USA

Received 23 March 1996; accepted 21 June 1996

ABSTRACT

Our major aim is to illustrate an approach for hindcasting or forecasting UV radiation (UVR, 280–400 nm) effects on *in situ* rates of aquatic primary production when field measurements do not include estimates of UVR effects. A composite of spectral field measurements is employed to model UVR-dependent rates of photosynthesis in diatom-dominated waters in a coastal region of the Southern Ocean. Assumptions, caveats and limitations of the modeling are discussed. Calculations begin with the 1991 Palmer Long Term Ecological Research (LTER) primary production and optical databases, from which daily integrated rates of carbon fixation in the absence of UVR are calculated as a function of depth for a 140 km transect line sampled between dawn and dusk of a single day (14 November 1991). The UVR measurements from the nearby NSF/OPP Polar Network at Palmer Station are used to determine ozone (O_3) concentration on the day of the transect, which is then employed in Madronich's (In *UV-B Radiation and Ozone Depletion* (Edited by M. Tevini), pp. 17–68. Lewis, Boca Raton, FL, 1993) spectral code to model daytime variations in surface spectral irradiances under clear sky conditions. These data are corrected for cloudiness and then combined with estimates of in-water UVR spectral attenuation coefficients, derived from *Icecolors '90* data, to estimate *in situ* light exposure for phytoplankton collected at different depths and locations. An absolute chlorophyll-specific biological weighting function (BWF), determined under natural solar light fields for Antarctic diatom communities and shown to be reproducible while differing from a laboratory diatom BWF and other *in situ* BWF determined for other phytoplankton assemblages, is combined with estimates of *in situ* UVR exposure to derive *in situ* estimates of chlorophyll-specific losses of carbon fixation due to UVR inhibition. By repeating calculations for every sampling site along the transect, we derive a spatial map of estimated UVR effects on primary production across the region. We repeat calculations for different O_3 concentrations expected during the austral spring over Antarctica and illustrate the O_3 dependency of UVB (280–320 nm) inhibition effects in near surface waters. We estimate ambient UVR reduced carbon fixation rates up to 65% in surface waters, depending upon location, down to undetectable levels at 36 m. Reducing stratospheric O_3 concentrations by 50% further inhibits near surface primary production by ≤8% and integrated primary production by ≤5%. Primary production was forced to subsurface maxima across the entire transect line in the presence of UVR.

INTRODUCTION

The approaches used to estimate and model aquatic primary production are many and varied, but all require, at some level, information on the characteristics of the underwater light field and the photosynthetic response of the phytoplankton. In the last decade, significant advancements have been made that couple optical models of light availability for aquatic photosynthesis with biooptical models of light-dependent rates of primary production. Input parameters in these production models are often measurable from space and allow a synoptic view of near surface primary production estimates over large space scales (1–6). Biooptical models have increased predictive accuracy over their predecessors, in part, because they rely upon better mechanistic understanding of relationships between photosynthetic available radiation (PAR,† 400–700 nm) and its ability to

*To whom correspondence should be addressed at: Marine Primary Production Group, Department of Ecology, Evolution and Marine Biology and the Center for Remote Sensing and Environmental Optics, University of California, Santa Barbara, Santa Barbara, CA 93106, USA. Fax: 805-893-4724;
e-mail: barbara@icess.ucsb.edu.

†*Abbreviations:* BWF, biological weighting function; Chl *a*, chlorophyll *a*; dpm, disintegrations per minute; DU, Dobson units; *E*, flux of light energy; FI, fractional inhibition; LT, local time; LTER, Long Term Ecological Research; O_3, ozone; PAR, photosynthetically available radiation (400–700 nm); P_{max}, photosynthetic potential; P_{PAR}, *in situ* photosynthetic carbon fixation rate in PAR-only light fields; P-I, photosynthesis–irradiance relationship; Q, photon flux density; RAF, radiation amplification factor; Sta, station; UVA, ultraviolet A radiation (320–400 nm); UVB, ultraviolet B radiation (280–320 nm); UVR, ultraviolet radiation (280–400 nm).

promote and regulate aquatic photosynthesis (7). When the spectral balance of PAR and its linkages to the spectral biology of phytoplankton are also included in field measurements and modeling efforts, the predictive accuracy of PAR-based production models increases further (7–9). For these and other reasons, there have been associated advances in sea-going instruments to facilitate underwater measurements of spectral PAR (10), spectral absorption of PAR by phytoplankton (7,11,12) and spectral PAR-based photosynthesis (11,12). Even with all these advances, most present PAR-based models of aquatic primary production are still largely based on exponential formulations for the underwater light field and basic photosynthesis *vs* irradiance (P-I) response curves, with limited dependence on other environmental conditions.

For Antarctica (13) and much of the rest of the globe (14,15), there has been a significant increase in the amount of solar UVB (280–320 nm) radiation reaching the earth's surface in recent years. The increase in UVB radiation is largely associated with loss of stratospheric ozone (O_3) (13–15). Changing O_3 concentrations have no direct effect on incoming PAR and little effect on incoming UVA (320–400 nm) radiation (16). Concern for the potential damaging effects of enhanced UVB radiation on plant life and short-term inhibitory effects on primary production, with unknown long-term consequences, has led us and others to field studies designed to quantify the spectral sensitivity of diverse Antarctic phytoplankton to fluctuating UV radiation (UVR) over the Southern Ocean (17–22). In doing so, it has become apparent that UVA and UVB inhibition of primary production may be overlooked in present measurements and large-scale models of aquatic primary production. Field measurements of P-I relationships, the basis of many productivity estimates, are generally made in the absence of UV radiation and even short incubations can provide sufficient time for partial or total release of phytoplankton from short-term UV effects on primary production (18). Thus, although PAR models of primary production may be accurate at estimating the potential primary production, they lack corrections for the loss of primary production due to inhibitory effects of UVR.

Thus, our interests include incorporating UVR effects into spectral models of PAR-based primary production such that the mechanistic linkage between changing UVR and rates of *in situ* carbon fixation are considered. However, to do so requires a large number of coordinated optical and biological measurements, including environmentally relevant spectral algorithms, *i.e.* action spectra or biological weighting functions (BWF), for UVR inhibition of carbon fixation for natural phytoplankton communities from diverse ecosystems. Although few such complete databases yet exist, we have recently published a BWF measured for springtime, Antarctic, coastal diatom-dominated communities and shown it to accurately predict UVR rates of primary production measured for the same community but on different days and under differing atmospheric O_3 conditions (18). We have observed that field-derived BWF are naturally variable and some considerations must be made in choosing among them, or others, in order to do reasonably accurate spectral modeling on time and space scales other than those for which they were determined (19–21). Here, we demonstrate that

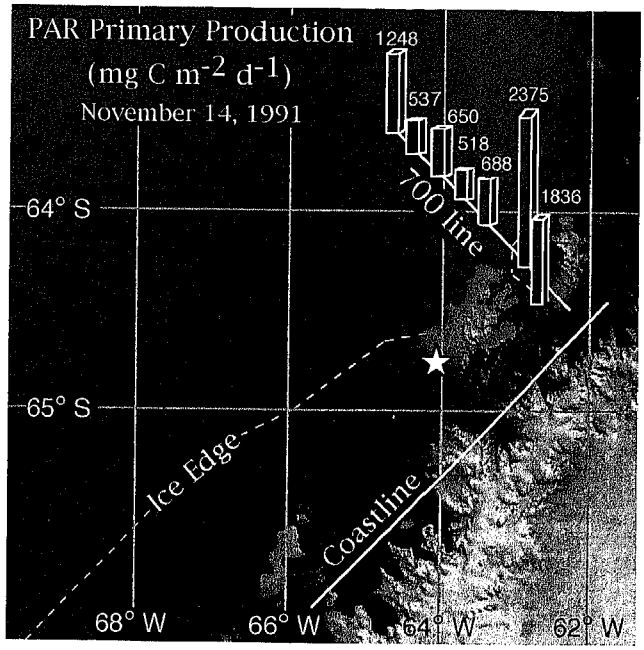

Figure 1. Location of the LTER 700 Line in waters west of Palmer Peninsula, Antarctica and Palmer Station (star) on the southwest side of Anvers Island. The coastal ice edge at the time of transect in November 1991 is shown by the dashed white line. The reference "coastline" for the LTER grid is also given. Numbering of transect stations start in Dallman Bay, on the northwest side of Anvers Island, with the station coastline being 700.020 and the furthest offshore station being 700.160. Different height columns at different transect stations represent PAR-dependent daily water column primary production (P_{PAR}, expressed as mg C m^{-2} day^{-1}). Primary production rates were determined from P-I measurements and corrected for daytime variations in both P-I parameters and in-water PAR (see text for details).

the BWF measured for Antarctic springtime diatoms in open water (18) was reproducible within the same diatom community on different days and then proceed to employ this BWF to spectrally model and hindcast UVR-dependent rates of primary production for regional space scales where similar diatom communities existed in Southern Ocean coastal waters. In doing so, we believe that our presentation of the data and data manipulation required for such spectral models, as well as a discussion of present constraints and inherent assumptions in trying to hindcast or forecast UVR effects, will benefit researchers making similar attempts in other aquatic environments where UVR is a significant environmental factor regulating primary production.

MATERIALS AND METHODS

Location and sampling of LTER stations. The Long Term Ecological Research (LTER) Program centered at Palmer Station, Antarctica, repeatedly surveys the characteristics of the waters west of the Palmer Peninsula. The oceanographic cruises are conducted seasonally aboard the R/V *Polar Duke* at defined stations within a defined 1000 km × 200 km LTER sampling grid (23). As part of the 1991 LTER spring survey, a minor diatom bloom was detected in Dallman Bay at sampling stations located on the designated 700 Line of the LTER grid (Fig. 1). The entire 700 Line runs 200 km perpendicular to the Palmer Peninsula, out from the coastline to the edge of the continental shelf. On 14 November 1991, we were able to transect the 700 Line from the nearest shore station 20 km from an arbitrary coastline (Fig. 1) out to a distance of 160 km offshore, *i.e.* from

station (Sta) 700.020 out to Sta 700.160. Intermediate transect stations on the 700 Line are located 20 km apart.

As each transect station was reached sometime between dawn and dusk on 14 November, a Biooptical Profiling System, BOPSII (16), was deployed to determine the physical, optical, chemical and biological properties of the water column. On upcasts of BOPSII, water samples were collected using 12 5 L Go-Flo bottles. In addition, Sta 600.040 (64°56.00'S, 64°24.000'W and 100 km SW of 700.040) and Sta 700.160 were sampled every few hours for a 24 h period on 7 and 15 November, respectively, in order to measure diel changes in photosynthesis and associated water column properties.

Pigmentation. For each BOPSII cast at each station, pigment samples were collected at eight or nine depths ranging from the surface down to a maximum depth of 200 m. Phytoplankton pigmentation was determined by HPLC, using modifications detailed in Moline and Prézelin (24). Pigment concentrations were measured on 1000 mL samples collected at each depth and filtered onto 0.4 μm 47 mm Nalgene nylon filters, which were frozen at −70°C for at least 2 h. Pigments were then extracted in 90% acetone at 0°C for 18 h. The acetone extracts were centrifuged and 300 μL of ion pairing solution was added to a 1 mL aliquot of the sample to increase the pigment resolution. A 350 μL aliquot of this mixture was injected into a Hitachi HPLC system (24), which was calibrated throughout over the field season with pigment standards provided by R. Bidigare.

PAR. Scalar irradiance (0.3–3.0 mm) at the ocean surface was continuously monitored using an Eppley pyranometer. The surface flux of PAR, $Q_{PAR}(O^+)$, was derived from scalar irradiance using the algorithm described by Baker and Frouin (25). At each station, attenuation of $Q_{PAR}(O^+)$ in the water column was derived from inwater measurements made with a profiling cosine sensor attached to BOPSII compared with simultaneous measurements made with a similar PAR sensor placed on deck. The daytime variations in $Q_{PAR}(O^+)$ were divided into 2 h intervals and then the mean value for each time interval was attenuated through the water column, utilizing each transect station attenuation coefficients for PAR, in order to provide estimates of in-water photosynthetic light availability for any time interval of that day at any station. These derived *in situ* PAR light field data are required to calculate *in situ* rates of PAR-only rates of primary production for any interval of the day.

PAR-dependent rates of primary production. Photosynthesis–irradiance relationships were measured on laboratory photosynthetrons (18), in the absence of UVR. Samples were collected at 6–10 depths at each station. A 30 mL aliquot of each sample was inoculated with $H^{14}CO_3^-$ to a final concentration of 9 μCi mL^{-1}. From each aliquot, 25 1 mL samples were dispensed into glass scintillation vials that were incubated in the photosynthetrons equilibrated to the *in situ* temperature for that sampling depth. Vials were incubated for 2 h at irradiances ranging between 4 and 1100 μmol quanta $m^{-2}s^{-1}$. At the end of the incubation, excess $H^{14}CO_3^-$ was removed from the samples using a heat-drying method (26), and dried samples were resuspended in 1 mL water and 3 mL fluor for determination of sample radioactivity. Volumetric PAR-only rates of primary production, P_{PAR} (mg C $m^{-3}h^{-1}$), were calculated from the measurements of the disintegrations per minute (dpm) of the sample and the total radioactive activity prior the incubation as described by methods in Parsons *et al.* (27). The P-I parameters quantifying the relationship between P_{PAR} and Q_{PAR} were derived using the equations of Neale and Richerson (28), such that

$$P_{PAR} = P_{max} \times \tanh\left(\frac{Q_{PAR}}{I_k}\right) \quad \text{for } Q_{PAR} \leq I_t \quad \text{and} \tag{1}$$

or

$$P_{PAR} = P_{max} \times \exp[-\beta(Q_{PAR} - I_t)] \times \tanh\left(\frac{Q_{PAR}}{I_k}\right) \quad \text{for } Q_{PAR} > I_t \tag{2}$$

where P_{max} is the light-saturated maximum rate of photosynthesis, I_k is the minimum light requirement for light saturation of photosynthesis ($=P_{max}/\alpha$), α is the light-limited photosynthetic efficiency, β is the efficiency of PAR photoinhibition and I_t is the minimum PAR requirement for photoinhibition. Equation 1 was employed where no photoinhibition was detectable and Eq. 2 was employed when photoinhibition at high Q_{PAR} was detectable. However, in the present study, the latter was rarely the case.

Because the transect stations were sampled at different times during a single day, estimates of the diel variation of Q_{PAR} and the P-I parameters at each station were desired in order to derive comparable (*i.e.* time-corrected) estimates of the rates of primary production across the transect line. Corrections for daytime variation in P-I parameters have been shown to be important for accurate estimates of PAR-dependent rates of primary production within the LTER region of the Southern Ocean (24). Following procedures first outlined by Prézelin *et al.* (26), primary production was monitored at two stations (600.040 and 700.160) by determining P-I relationships for samples collected every 2–4 h at 6–10 depths. These derived P-I parameters were normalized to the maximum daytime values and interpolated to a common time and depth grid of 2 h over 24 h and for 10 m intervals from the surface down to 100 m. Results from Sta 600.040, where diatoms were dominant, were used to derive diel patterns of P_{PAR} from instantaneous measurements made for diatom communities at LTER Sta 700.020 to 700.060. The rationale was based upon observations that Antarctic diatoms collected in the spring and summer in the LTER grid have been shown to display similar patterns of daytime variations in primary productions (24). Diel patterns of primary production derived from studies at Sta 700.160, where mixed phytoplankton communities were evident (see below), were used to derive daytime patterns of P_{PAR} from instantaneous measurements made at Sta 700.080 to 700.160 during the 700 Line transect on 14 November. For each station and at each depth, daily rates of primary production P_{PAR} (mg C m^{-3} day^{-1}) were determined by trapezoidal integration of the daytime variations in rates of primary production P_{PAR} determined for 2 h intervals between dawn and dusk.

Determination of simulated in situ *BWF for UVR inhibition of PAR rates of primary production.* Experimental procedures for determination of the BWF used in the present calculations are detailed in Boucher and Prézelin (18). Briefly, replicate BWF for diatom-dominated communities were measured on 14 and 16 September 1993, for natural phytoplankton communities collected in the waters off Palmer Station, Antarctica. The BWF were determined in outdoor simulated *in situ* incubators (29), thereby assuring that samples were exposed to the natural fluctuations in the solar light field over the day. Replicate samples, incubated with $H^{14}CO_3^-$, were exposed to six different spectral light treatments where different combinations of long-pass filters selectively removed increasingly larger portions of the UVR spectrum. Spectrally integrated Q_{PAR} was monitored continuously using a Biospherical 185B photometer placed next to the outdoor incubator and 5 min averages were recorded on a Licor 1000 datalogger. In addition, the NSF/OPP polar UV network at Palmer Station (30) provided light data from which surface spectral irradiance from 290 to 700 nm could be derived for each hour of incubation. Light exposure for samples placed in the outdoor incubators was calculated by multiplying these irradiance spectra by the transmission spectrum of the different spectral incubator lids and that of the transparent Whirlpac bags in which samples were incubated. The BWF were derived from measurements of the time course of carbon uptake over a single day in each of the six spectral light treatments (18). Duplicate samples were removed every hour from 10:00 to 18:00 local time (LT) on 16 November. On 14 November, replicate surface samples were incubated from 08:00 to 17:00 LT and the BWF determined for samples collected following the 9 h incubation. Recovered samples were fixed with 0.5% formalin and gently filtered onto a 0.4 μm Nuclepore filter and then rinsed with filtered seawater. Sample dpm were determined and corrected for dark fixation.

For each sampling time, the amount of carbon fixed in the sample exposed to PAR-only treatment was used as a reference to compute the fractional inhibition (FI) by UVR of PAR-dependent rates of production in the other spectral light treatments (PAR + UVR), such that

$$FI = 1 - (P_{PAR+UVR}/P_{PAR}). \tag{3}$$

We assumed that the fractional inhibition, FI, over a time interval can be expressed as a function of the average UV irradiance ($E_{UVR}[\lambda]$, in W m^{-2}) which impinges on the phytoplankton com-

munity inside the incubator and the BWF ($\epsilon[\lambda]$, $[W\ m^{-2}]^{-1}$), representing the spectral sensitivity of the organism to such radiation, such that

$$FI = \Sigma_{UVR} E_{UVR}(\lambda)\epsilon(\lambda)d\lambda \quad (4)$$

Because FI is derived from broadband measurements, $\epsilon(\lambda)$ cannot be mathematically derived from Eq. 4 alone. However, the method outlined by Rundel (31) can be used to extract the spectral dependency of the BWF from knowledge of the several broadband FI. The accuracy of this deconvolution technique increases with the number of filters used and depends on the distribution along the UV region of the spectrum of the transmittance cut-offs of the filters. To compensate for the limited number of affordable and suitable long-pass filters, we concentrated the highest resolution in the UVB region of the spectra, where the slope of the BWF has been shown to vary the most for other plant photoprocesses. Therefore, averaged inhibitions over the day were combined with spectral irradiance in each treatment to derive the daily integrated BWF employing a modified version of the exponential decay function of Rundel (31). In the recent study of Boucher and Prézelin (18), the predictive accuracy of the derived diatom-dominated BWF was tested and proved predictively robust within the same community under different stratospheric O_3 conditions.

Modeling spectral UVR during the 1991 LTER cruise. The UVR-PAR spectral code of Madronich (14) was employed to model surface spectral irradiances at the ocean surface for 14 November for the mean latitude of the 700 Line. To derive the full UVR-PAR spectral irradiances likely at the surface under clear sky conditions, it was necessary to have an input estimate of the stratospheric O_3 concentrations that largely determine the UVB radiation reaching the ocean surface. The archived UV measurements made at the nearby NSF/OPP Polar Network at Palmer Station indicated that midday O_3 concentrations were 318 Dobson units (DU = matm cm) on 14 November 1991. Clear sky estimates of UVR-PAR spectral irradiances at the earth's surface were modeled for every hour on the hour of measurable daylight. To compensate for actual cloud cover, the modeled clear sky spectral irradiances of Q_{PAR} were normalized to surface Q_{PAR} derived from Eppley measurements made on the ship from dawn to dusk on the transect day (see above). The normalization required to match modeled clear sky and measured shipboard Q_{PAR} was then used to normalize modeled spectral Q_{UVR} and estimate *in situ* Q_{UVR} at the ocean surface. One of the necessary assumptions is that cloud attenuation is independent of wavelength over the UVR and PAR region of the solar spectrum. Recent work (Madronich, personal communication) has shown that, to a first approximation, this holds true under uniformly overcast skies that are typical conditions in Antarctica and for 14 November 1991 along the 700 Line.

Whereas data on in-water attenuation of broadband Q_{PAR} are needed to derive P_{PAR} estimates of *in situ* primary production from depth-dependent P-I relationships (see above), estimates of the UV inhibition of P_{PAR} from the use of BWF require in-water spectral light data. However, there are a lack of published in-water spectral UV light data for the Southern Ocean. We assume that spectral vertical attenuation coefficients, $K_d(\lambda)$ (Fig. 2), derived from six light profiles measured during *Icecolors '90* in the austral spring 1990, are also applicable to the present study. Some justification came from observations that phytoplankton biomass in the upper water column (0–36 m) for both cruises was very similar and low in concentration, *i.e.* ranging from 0.8 to 1.2 mg chlorophyll *a* (Chl *a*) m^{-3}. Additional assurance comes indirectly from estimates of broadband UVB attenuation coefficients derived by Vernet *et al.* (32) for various sites along the Palmer Peninsula in 1988, which suggested an average value of *ca* 0.12 m^{-1} was appropriate for Chl *a* + pheopigment concentrations of 0.4 mg Chl *a* m^{-3}. Although the linear correlation was not good, and related to photophysiological variability between different phytoplankton taxon, there was a 4-fold variation in their UVB attenuation coefficients with about a 19-fold increase in Chl *a* + pheopigment concentrations. Assuming linearity and not correcting for pheopigments (which we have found to be rarely abundant in these waters), the data of Vernet *et al.* (32) would suggest a broadband estimate of K_d for UVB wavelengths of *ca* 0.17–0.21 m^{-1} for biomass concentrations measured along our transect line in 1991. These rough estimates compare well with the spectral $K_d(\lambda)$ derived from the *Icecolors '90* data (generously provided by R. C. Smith) for UVB wavelengths and employed here to model in-water UVR light fields (Fig. 2). Furthermore, absorption by dissolve organic substances was likely to be low, as it was in the *Icecolors '90* cruise (unpublished data), given the acceleration of springtime phytoplankton growth had just begun and the area was largely ice free. Thus, we estimated the daytime pattern of flux of spectral UVR at depth ($E_{UVR}[\lambda,z]$) at each transect station from the knowledge of the surface UV irradiance ($E_{UVR}[\lambda,O^+]$) as

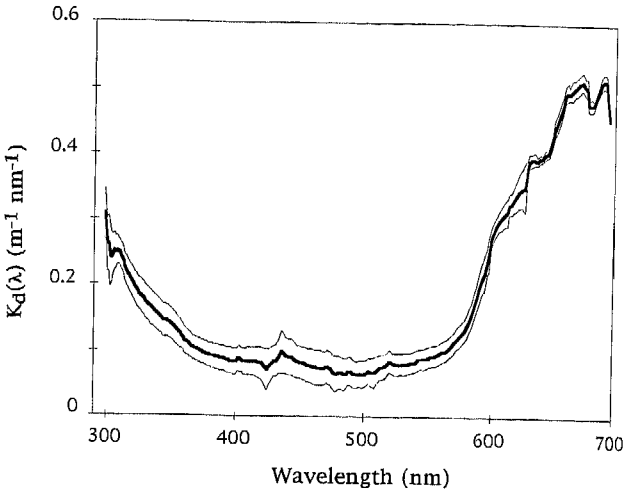

Figure 2. Spectral vertical attenuation coefficient ($K_d[\lambda]$) determined for the *Icecolors '90* expedition in the marginal ice zone west of the Antarctic Peninsula. The error represents 1 standard deviation around the mean ($K_d[\lambda]$) for six profiles from 0 to 36 m. Light data for these derivations were generously provided by R. C. Smith.

$$E_{UVR}(\lambda, z) = E_{UVR}(\lambda,O^+)e^{-Kd(\lambda)z} \quad (5)$$

UVR-dependent daily rates of primary production. By combining estimates of *in situ* UVR exposure $E_{UVR}(\lambda)$ with the absolute Chl-specific BWF $\epsilon(\lambda)$ determined in the field for similar diatom communities, we derive estimates of Chl-specific losses of carbon fixation due to UVR inhibition for *in situ* conditions. Formulation was identical to that in Eq. 4 and estimates were made for each hour of the day at each station and interpolated to derive daily estimates of UVR inhibition on *in situ* rates of primary production.

RESULTS AND DISCUSSION

Environmental optics

Studies of the impact of UVR climatology in natural ecosystems require understanding of environmental optics and use of somewhat different experimental approaches than those more commonly used in laboratory UVR studies (29,33–36). Even though UVR reaching the earth's atmosphere extends down to wavelengths approaching 200 nm, radiation below 295 nm rarely reaches the earth's surface (Fig. 3). All of the UVC radiation (200–280 nm) is attenuated very rapidly by oxygen (O_2) molecules in the top portion of the earth's atmosphere. The sharp cut-off in spectral irradiance at the lower end of the UVB region (280–320 nm) (Fig. 3) is attributed to O_3 absorption (14). The O_3 molecule absorbs selectively in the UVB region: the absorption cross section decreases exponentially in wavelengths longer than 260 nm to near negligible values in the higher UVA region of the spectra (320–400 nm) (37). The impact of changing midday O_3 concentrations on surface spectral irradiances at the Antarctic study site is illustrated in Fig. 3. As O_3 levels decline, shorter wavelengths of UVB radiation reach the

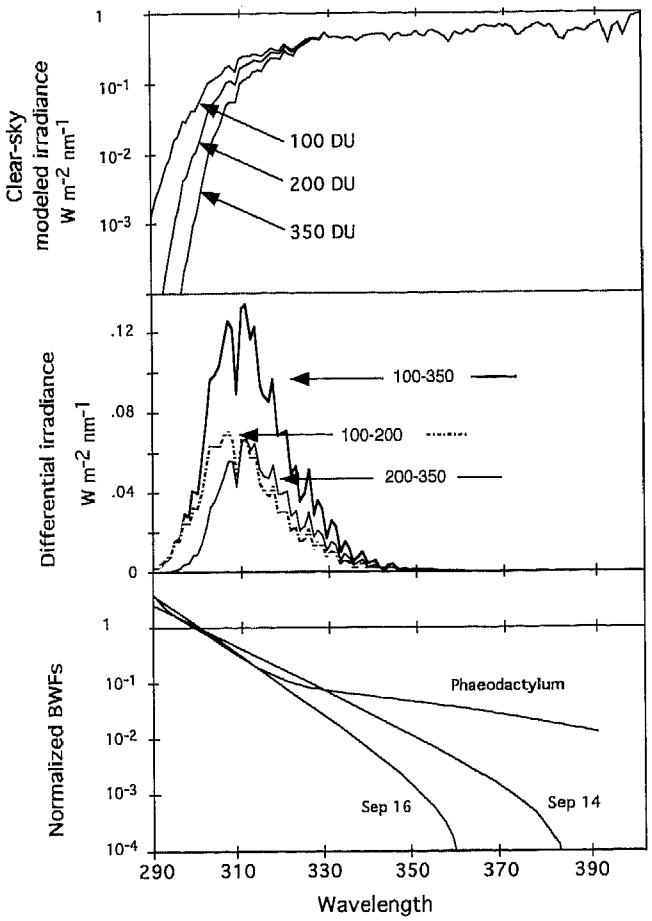

Figure 3. Top: Spectrally modeled clear sky UV irradiances that would reach the ocean surface at solar noon on 14 November of any year at the mean latitude of the 700 Line, as estimated by the UV-PAR code of Madronich (15). A comparison is made of variations in spectral UV irradiances as a function of changing overhead O_3 concentrations, ranging from 350 to 100 DU. Middle: Illustration of O_3-dependent increases in clear sky UV spectral irradiances that would result at the same site and time of year from a reduction of O_3 concentrations from 350 to 100 DU (the 100–350 line), from 350 to 200 DU (the 200–350 line) and from 200 to 100 DU (the 100–200 line). Bottom: The simulated *in situ* BWF for UV inhibition of carbon fixation measured for diatom-dominated communities at Palmer Station on 16 September 1993 (18) and used to hindcast UV effects in the present study. This BWF is compared with a BWF measured in the same water mass 2 days earlier and with a BWF for a laboratory culture of the temperate diatom, *Phaeodactylum tricornutum* (48).

earth's surface in greater quantities and the spectral enhancement of the light field depends largely on the degree of change in O_3 concentrations. It is also known that sun angle and latitude, as well as several other factors, combine to further influence the O_3-dependent spectral irradiances at any given time and location (14). In the Antarctic springtime, very large and sudden fluctuations in incident UVB can occur as the O_3 hole rotates overhead (16). Thus there is an O_3-dependent effect on the UVB : UVA : PAR ratio of incident light fields that drives the polychromatic biology of marine phytoplankton (16,29,38). Independent of O_3 concentrations, daytime changes in solar zenith angle drive daytime variations in the UVB : UVA : PAR spectral balance, with UVB : UVA ratios several-fold higher in the middle of the day than at either dawn or dusk (29) (also see below). Thus, the environmental spectral light field is ever changing in magnitude and spectral balance and is not easily mimicked in laboratory settings (33,38).

Historically, the detrimental effects of UVR on marine environment were thought to be confined to the surface (39). The penetration of UVR to significant depths in the water column and its potential negative effects on living organisms had, however, been demonstrated very early (40,41). In 1992, a newly designed and much more sensitive underwater UVR spectroradiometer detected UVB radiation at depths greater than 70 m in clear waters of the Southern Ocean (16). Since then, UVB penetration in other bodies of fresh and marine waters have been better documented (42,43). Thus, there is no longer scientific doubt that UVR, including O_3-dependent UVB radiation, penetrates to ecologically significant depths in aquatic ecosystems.

In situ BWF for Antarctic phytoplankton

The degree to which different aquatic organisms are affected by a given amount of UVR varies between organisms, their life history and other factors that affect the quality of their habitats (34–36). For phytoplankton, UVB effects depend upon a combination of factors including their position in the water column, their natural or photoinduced protection, the sensitivity of their molecular structures and their repair abilities (16,44). With the advent of global O_3 depletion (15), action spectra have started to be used as BWF to more accurately assess the effect of the associated increase in UVB radiation on various biological and ecological processes (45,46). However, *in situ* BWF availability is limited and we lack knowledge of the applicability of various BWF to specific environmental conditions. Present spectral modeling of environmental UV effects must therefore be done with caution and predicted consequences must be appropriately applied to efforts to predict ecosystem responses to changing UVR climatology.

In Fig. 3, we present the two *in situ* BWF derived for diatom-dominated communities collected from surface waters at Palmer Station (Fig. 1) during September 1993. The BWF determined for 14 September and 16 September closely resemble each other, with both lying well within overlapping error estimates for each curve (19,21). The relative chemotaxonomic algal pigments and relative phytoplankton biomass, as well as hydrographic and properties of the water samples, compare well for diatom-dominated communities collected for BWF determinations at Palmer Station on the SW side of Anvers Island (18) and field transect samples collected from Dallmann Bay on the NW side of Anvers Island (Fig. 1) (see below). The details of the derivation of 16 September BWF are presented in Boucher and Prézelin (18), as well as results showing that this BWF accurately predicted the UVR-dependent rates of *in situ* primary production when the same community was sampled 1 week earlier under different stratospheric O_3 conditions. On 16 September 1993, the daily *in situ* BWF (Fig. 3), in combination with the UVR light field measured for that day at the sampling site, predicted a 34% reduction in average carbon fixation, with 15% attributable to UVB radiation and 19% attributable to UVA radiation (18).

Additional *in situ* BWF were determined during the austral spring 1993 for phytoplankton assemblages other than those dominated by diatoms and varied widely in their relative spectral sensitivities to UVA and UVB radiation (19–21). The hydrographic and taxonomic conditions for these other BWF determinations made them less appropriate for use in the present spectral modeling application. These observations however suggest that the accuracy of UV spectral model predictions will depend upon the matching of appropriate BWF with the appropriate field conditions and that the use of constant BWF to predict effects on very large time and space scales (47) may lead to sizable, but presently unknown, errors.

Of the three BWF thus far reported for UVR inhibition of marine diatom photosynthesis (Fig. 3), the *in situ* BWF for Antarctic communities are markedly different from the one laboratory BWF reported for a culture of a temperate diatom, *Phaeodactylum* sp. (48). However, on an absolute basis, the two daily integrated *in situ* BWF were very similar. At the O_3-dependent wavelength of 310 nm (Fig. 3), both BWF predicted that exposure to 1 J m^{-2} day^{-1} of quanta would cause a loss of 6–8 × 10^{-3} g C m per g Chl a^{-1} day^{-1} (19). At 350 nm, in the UVA portion of the solar spectrum, 1 J m^{-2} day^{-1} of quanta would cause a loss of *ca* 5 × 10^{-5} to 2 × 10^{-6} g C m per g Chl a^{-1} day^{-1}. At wavelengths >370 nm, inhibition of photosynthesis by UVA was negligible and UVA actually enhanced rates of primary production. Increased *in situ* primary production and phytoplankton growth by exposure to UVA radiation has not been universally observed but often enough to suggest that, like UVB radiation, biological inhibition by UVA radiation is highly variable in natural ecosystems (*cf.* 13,22). Universal conclusions regarding the relative importance of UVB *vs* UVA radiation in regulating Antarctic aquatic primary production (47) are not warranted at present.

The BWF presented in Fig. 3 are normalized at 300 nm, the wavelength below which little UVR reaches the earth's surface and penetrates the upper water column. The normalized comparison is useful for highlighting the relative differences in UVB and UVA sensitivities for different BWF and for comparative determinations of their sensitivities to changes in O_3 climatology. The comparison shows that the laboratory culture was much more sensitive to UVA radiation than the field communities. Utilization of the laboratory BWF to predict UVR effects in the Southern Ocean, as recently attempted for the entire Southern Ocean (47), would result in conclusions that UVA was by far more inhibitory to marine photosynthesis than UVB radiation and, thus, that O_3-dependent increases in UVB would have minimal impacts on the ambient levels of UVR-dependent rates of carbon fixation in the Southern Ocean. Had one of the other BWF been used in these regional scale estimates, a different view might have been taken as the relative UVA sensitivity of the *in situ* BWF for Antarctic coastal diatoms on 14 and 16 September were at least two orders of magnitude lower than that measured for the laboratory culture (Fig. 3). It is possible that a patchwork of BWF applied on different time and space scales, and matched to the time and space scales of changing phytoplankton dynamics in different aquatic ecosystems, may be required to get an accurate assessment of UVR effects on Southern Ocean primary production.

Lastly, the sensitivity of a given photoprocess to a decrease in O_3 concentration can be quantified by a single parameter, the radiation amplification factor (RAF). The RAF is a measure of the relative increase in biologically effective UVB radiation for a given level of O_3 reduction. It has recently been mathematically described for large variation in O_3 concentration by Madronich (14) using the power formulation:

$$\frac{I_i}{I_{360}} = \left(\frac{N_{360}}{N_i}\right)^{RAF} \quad (6)$$

where I_i and I_{360} are the inhibition corresponding to ozone concentration of i DU (N_i) and 360 DU (N_{360}). Madronich *et al.* (49) have also compiled a list of BWF for a variety of photochemical and photobiological processes, while pointing out that RAF themselves vary with changes in overhead O_3 concentrations and solar zenith angles. For the same set of conditions (midsummer, 305 DU, at a fixed latitude of 30°N), the RAF derived from the BWF for the laboratory diatom culture was 0.3 (49), while the RAF for the natural Antarctic diatom-dominated assemblages was 0.8 for the BWF determined on 16 September 1993 (49) and 0.6 for the BWF determined on 14 September 1993 (19,21). Thus, for every 10% drop in stratospheric O_3, the *in situ* diatom-dominated communities in surface waters would experience a 6–8% decline in rates of carbon fixation for the conditions defined in the calculations; values would, of course, vary with a change in conditions. However, under the same conditions, the natural diatom communities would be at least twice as sensitive to changes in O_3 climatology than would have been predicted from use of the BWF results from the *Phaeodactylum* study. The difference in the predictive outcome of the use of different BWF further supports the view that data for ecosystem modeling of UVR effects should either come from the ecosystem being considered (13,16,18,21,22,29,33–36,38) or at least a thorough consideration of the limitations of using any BWF over a range of ecosystems should be included in estimates of possible predictive errors.

Presence and dominance of diatoms along the LTER 700 line

Chlorophyll *a* is used as an indicator of phytoplankton biomass and key carotenoid pigments are used as taxonomic markers for different phytoplankton classes (Fig. 4). Plotting the distribution of the *in situ* concentration of these pigments allows analyses of the spatial variability in phytoplankton community composition and can be used to define further the association of specific phytoplankton assemblages with various ocean regimes. It is because of the dominance of diatoms on the 700 Line that this particular transect was selected to apply an *in situ* BWF derived for diatom-dominated natural communities for the purpose of hindcasting UVR effects on PAR-dependent rates of primary production in Antarctic coastal waters.

Plant biomass was relatively low over the entire 700 Line but showed a high variability in distribution, both on the vertical and horizontal scale (Fig. 4). Highest Chl *a* biomass (*ca* 0.8 mg m^{-3}; Fig. 4), as well as phytoplankton beam attenuation (50), was found in Dallmann Bay (700.020–060,

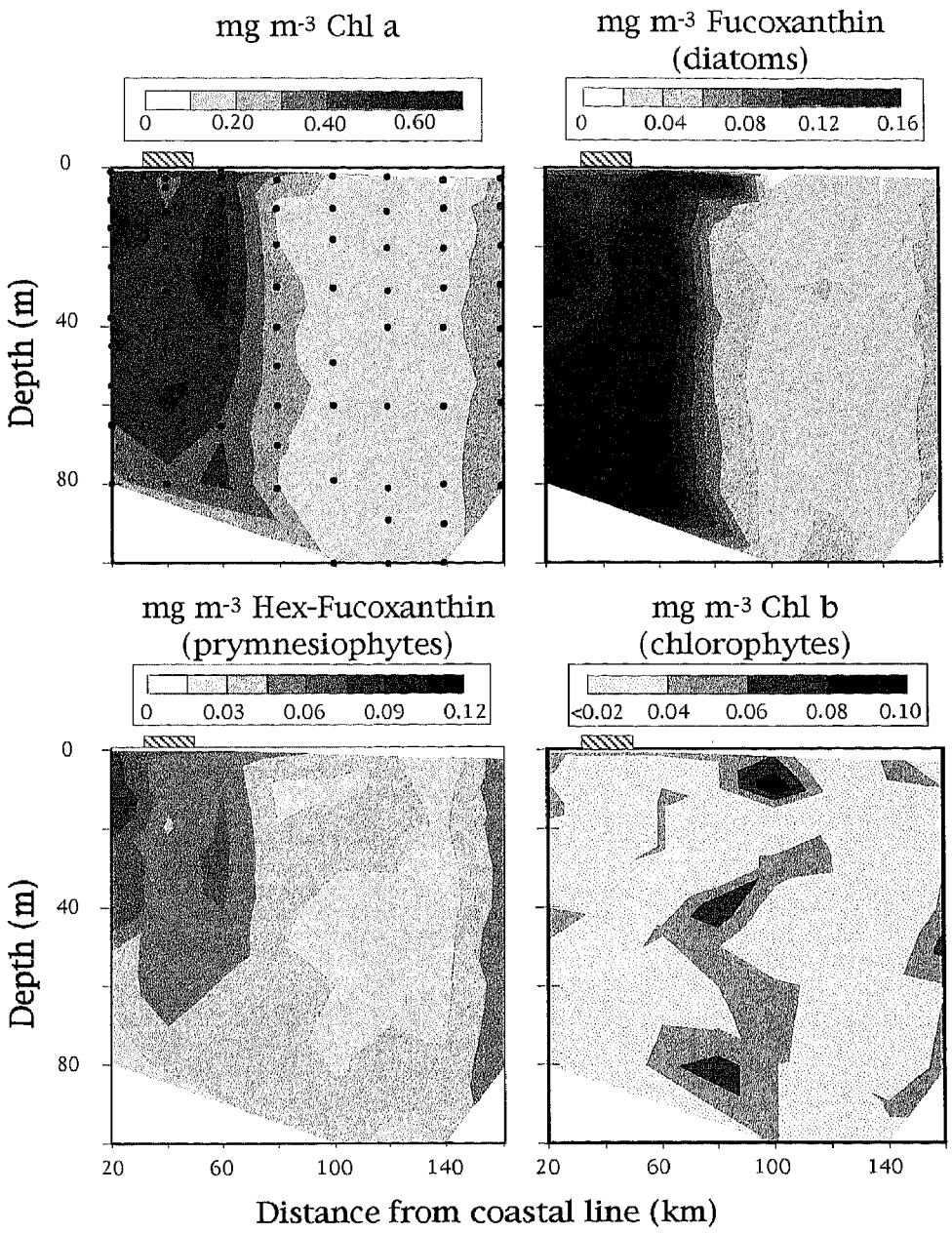

Figure 4. Contour plots of the spatial distribution of the four major phytoplankton pigments along the LTER 700 Line on 14 November 1991. Pigment concentrations are given in mg m^{-3} and the phytoplankton class that each pigment chemotaxonomic marker represents is given in parentheses. Pack ice coverage (slashed bar) is indicated at the top of each panel and depths of sampling are shown by the closed circles in the contour of Chl *a* biomass in the top left panel.

Fig. 1). Here, diatoms dominated the phytoplankton assemblages as indicated by the high fucoxanthin concentration in these shallow coastal waters (Fig. 4). Both the vertical and horizontal distribution of high biomass at subsurface and around the loose pack ice patch (station 700.040) support the hypothesis that the minor diatom bloom was induced by an increase in water-column stratification brought upon by some springtime melting of sea ice (24,51). This conclusion is supported by evidence that the −1°C isotherm shallowed from >100 m at offshore stations to *ca* 60 m at these nearshore stations, where the water column was characterized by a highly stratified halocline around 60–70 m (50). The vast majority of the distribution of Chl *a* and diatom-dominated biomass in the entire water column from station 700.020 to 700.060, as well surface samples at 700.080, were associated with this low density and salinity water not found further offshore.

Whereas a significant portion of the phytoplankton communities at all stations and depth was attributable to diatoms, their dominance gave way to other groups of phytoplankton at stations further from the coast where the upper water column was no longer highly stratified. The low biomass (<0.2 mg Chl *a* m^{-3}) intermediate open water stations (700.080 and 700.100) consisted of mixed phytoplankton communities comprised of variable ratios of diatoms, prymnesiophytes (Hex-fucoxanthin), chlorophytes (Chl *b*) and coccolithophorids (data not shown) (52). Such assemblages are characteristic of diatom postbloom waters (53), suggesting that a marginal ice edge bloom might have been previously advected out by the strong westerly winds. This suggestion is

supported by hydrographic data discussed above and further detailed elsewhere (50).

PAR-dependent rates of primary production

Many field measurements and biooptical models of aquatic primary production (54) do not include consideration of UVR effects on rates of primary production. The result has been that PAR-dependent models of primary production fairly well predict simulated *in situ* or *in situ* measurements in the absence UVR (7,55) and provide a good basis for incorporating UVR effects modeled separately. The commonly employed method of determining P-I relationships using PAR-only laboratory incubators provides estimates of the potential productivity in the absence of UVR if the field sample is known to have recovered from ambient UVR inhibition during the incubation period. Comparisons of carbon fixation rates of water samples incubated simultaneously in *in situ* UVR moorings and/or simulated *in situ* deck incubations with those incubated in bluegreen light laboratory photosynthetrons showed that Antarctic phytoplankton communities appear to recovery fully from UVR inhibition on our photosynthetrons during 1.5–2.5 h incubations (18,29). Even though this might not hold true under other conditions, we are confident for the present data set that the photosynthetron measurements did provide for accurate estimations of PAR-only rates of primary production on the 700 Line.

The LTER 700 Line was transected between dawn and dusk of a single day in November 1991. Because we assumed that the surface insolation was approximately the same at all stations along the transect for that day, we began the biooptical modeling of *in situ* primary production by first constructing the PAR light field from shipboard measurements provided by R. C. Smith. From Fig. 5a, it can be seen that on 14 November 1991, when daylength was about 16 h long, surface PAR fluctuated over the day in response to variable cloudiness. The depth to which 1% PAR penetrated the water column (*i.e.* the depth of the euphotic zone for primary production) varied between stations, ranging from *ca* 100–160 m (50). The observation of deep euphotic zones supports the view that the water columns at different stations along the transect were quite transparent to incoming solar irradiance and that spectral attenuation coefficients for PAR and UVR would not differ greatly between stations. This is an important observation for later calculations of the UVR in-water light fields where we assumed, out of necessity, that the spectral attenuation coefficients for UVR (Fig. 2) were constant at all locations along the transect.

Photosynthesis–irradiance relationships, determined throughout the upper 100 m of the euphotic zone at each transect station, were combined with knowledge of the in-water PAR light field to derive instantaneous rates of *in situ* primary production (see Eq. 1 and 2). In addition, on two occasions (stations 600.040 and 700.160), the ship was maintained on station for 24 h and P-I parameters were determined every 2–4 h at 6–10 depths. Examples of the diel periodicity in PAR-only determination of P_{max} for surface and 20 m samples for these two stations are presented in Fig. 5b. Other P-I parameters were also determined to have a diel periodicity that differed with depth and depended upon whether the community was dominated by diatoms (station

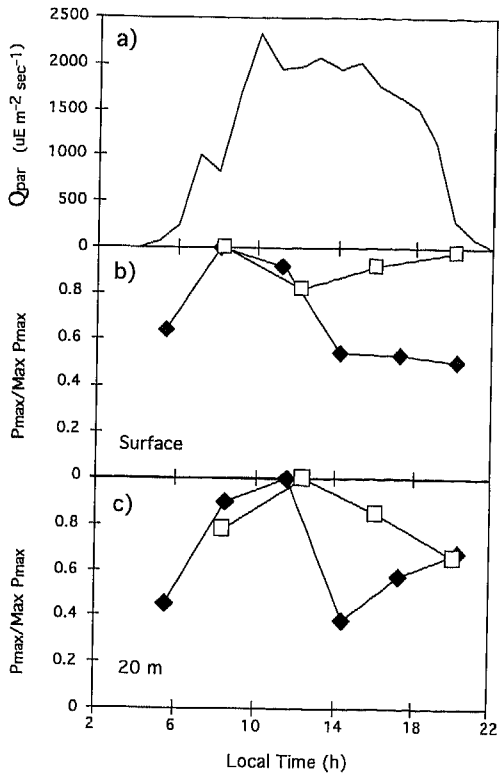

Figure 5. Daytime variations in (a) incident PAR at the ocean surface along the LTER 700 transect line on 14 November 1991; (b) the ratio of instantaneous P_{max} to maximum daily P_{max} for diatom-dominated (closed diamonds) and mixed phytoplankton (open squares) communities sampled in surface waters of LTER stations 600.040 and 700.160 on 7 and 15 November 1991, respectively; (c) same as b but for 20 m phytoplankton communities.

600.040) or mixed phytoplankton communities (station 700.160). Because it has been shown that consideration of daytime variations in P-I parameters is a necessary step in accurate prediction of *in situ* primary production in LTER coastal waters (24), we here used the diel patterns of primary production to time-correct instantaneous measurements of PAR-only rates of primary production along the LTER 700 Line. As a result we were able to estimate *in situ* PAR-only production rates for any time of day and location along the transect on 14 November. We used this discrete interval data to calculate PAR-dependent rates of *in situ* primary production for the entire day at each location (Fig. 5) and for the entire water column at each station (Fig. 1). The time-corrected production data were also used to model UVR effects on marine photosynthesis for different intervals of the day (see below).

The P_{PAR} along the transect was highly variable and closely reflected the water column integrated biomass distribution (compare Fig. 4 and Fig. 6). In Dallmann Bay (700.020–060), the production maximum was at 10–25 m and coincident with a subsurface Chl *a* maximum (Fig. 5, top). At Station 700.100, production was maximal in the surface waters. At Station 700.120, the production maximum was at 60 m nearer the base of the euphotic zone. At Sta 700.160, the production maximum was at the surface and similarly productive waters extended down the water column about 40–50 m.

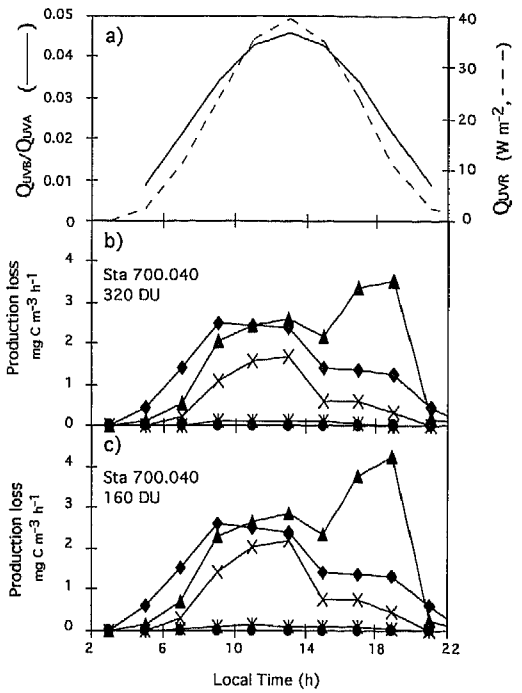

Figure 6. Comparison of daytime variations on 14 November 1992, at the LTER study site, for (a) spectrally modeled incident UVR (dashed line) and UVB: UVA ratio (solid line) when stratospheric ozone concentrations were 318 DU; (b) estimated hourly losses in carbon fixation, due to UVR inhibition, at the diatom-dominated station (700.040) as a function of depth (surface, closed diamonds; 10 m, closed triangles; 20 m, x's; 30 m, stars; and 40 m, closed circles) and spectrally modeled with an ozone concentration of 320 DU; (c) same as b but spectral-modeled estimates of UVR-dependent carbon losses per hour are based on a stratospheric ozone concentration of 160 DU.

The coastal diatom community in Dallmann Bay was most productive with daily integrated carbon uptake averaging about 2 g m^{-2} day^{-1} (Fig. 1). These values are about twice as high as prebloom diatom production measured at Palmer Station about a week later and much less than the 7 g C m^{-2} day^{-1} measured at Palmer Station when the seed diatom population developed into a major local bloom at Palmer Station in mid-December 1991 (24). Primary production in the *Phaeocystis*-dominated communities offshore approached 1.3 g m^{-2} day^{-1} and the intermediate region of mixed communities were the least productive with uptake numbers below 0.6 g m^{-2} day^{-1}.

UVR effects on *in situ* primary production

Figure 6a illustrates the daytime variations in UVR spectrally modeled for the LTER study site on 14 November. The flux of UVR varied *ca* five-fold over the day and peaked at solar noon (13:00 LT). The figure also illustrated that the ratio of UVB to UVA radiation in the natural light field also varied *ca* five-fold over the day. Thus the biological effectiveness of UVB inhibition of primary production would increase relative to the biological effectiveness of UVA inhibition during the midday hours, if the phytoplankton spectral sensitivity to UVR did not change over the day. As mentioned above and elsewhere (29,57), there is reason to believe that phytoplankton do alter their spectral sensitivities

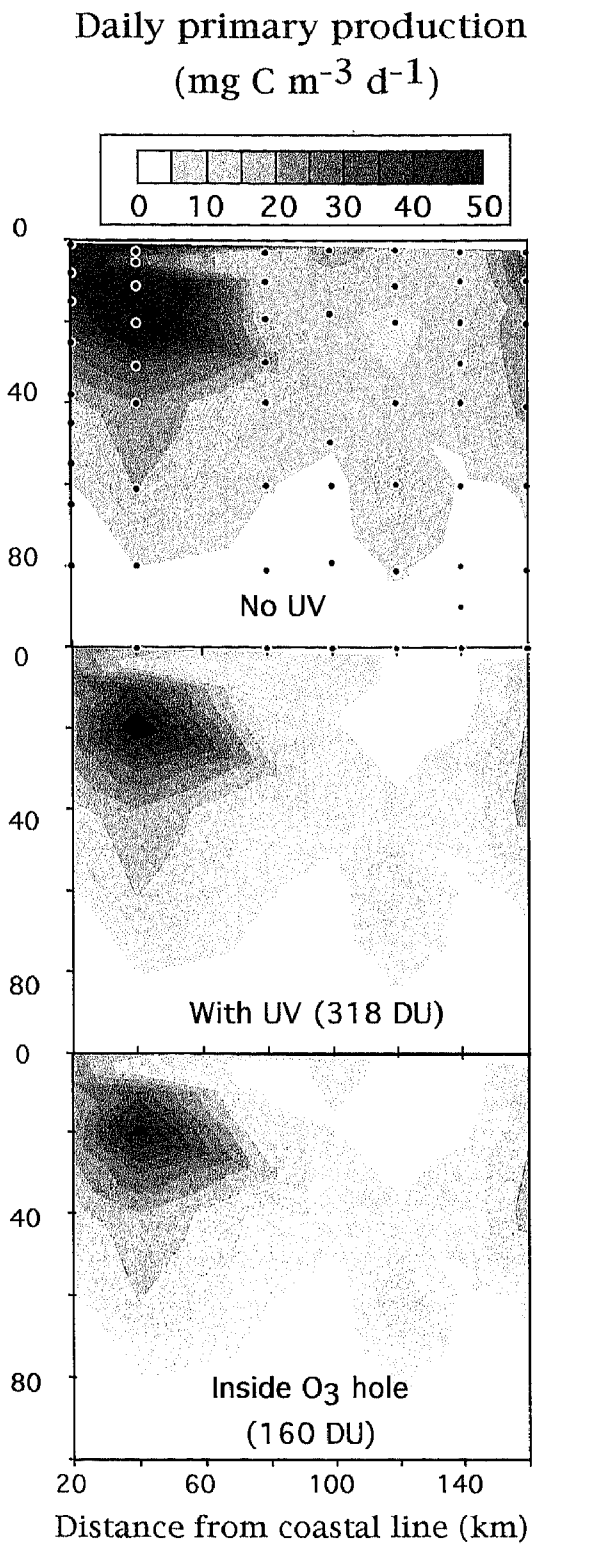

Figure 7. Contour plots of the spatial distribution of daily primary production along the LTER 700 Line on 14 November 1991. Values were corrected for daytime variations in *in situ* production and inwater spectral light fields. Production values are given in mg $m^{-3}day^{-1}$. Top: Production values for PAR-dependent rates of carbon fixation in the absence of UVR. Middle: Production values corrected for estimated UV inhibition modeled for ambient O_3 concentrations of 318 DU and corrected for cloudiness. Bottom: Estimated values for PAR-dependent rates of carbon fixation when ambient O_3 concentrations at the study site were reduced to 160 DU.

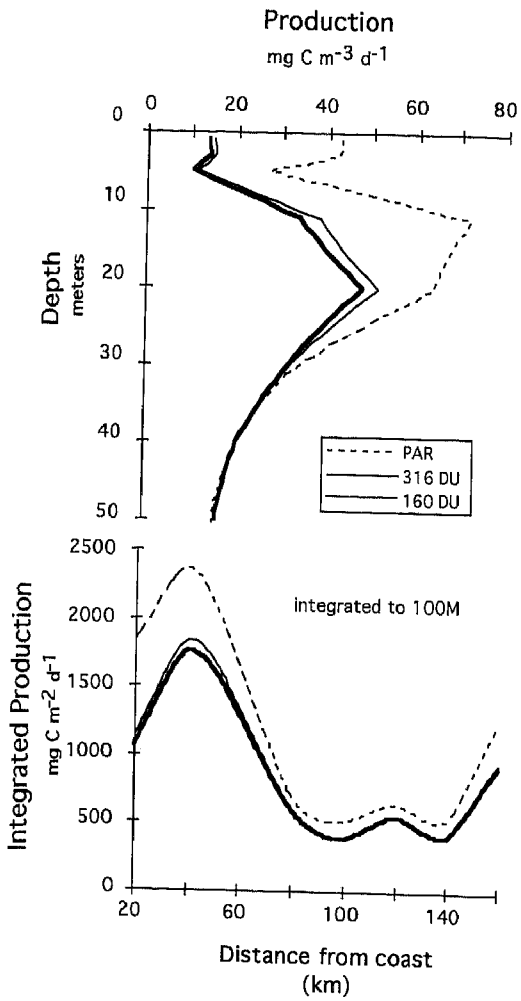

Figure 8. Comparison of the PAR-dependent and UV-dependent estimates of daily primary production (top) for a depth profile within the diatom-dominated communities of Dallman Bay at station 700.040 and (bottom) for integrated values for the upper 100 m of different transect stations occupied on the LTER 700 Line on 14 November 1991. The UV-dependent estimates are compared for ambient O_3 concentrations of 318 DU and for a reduction of O_3 to 160 DU as described in Figure 7.

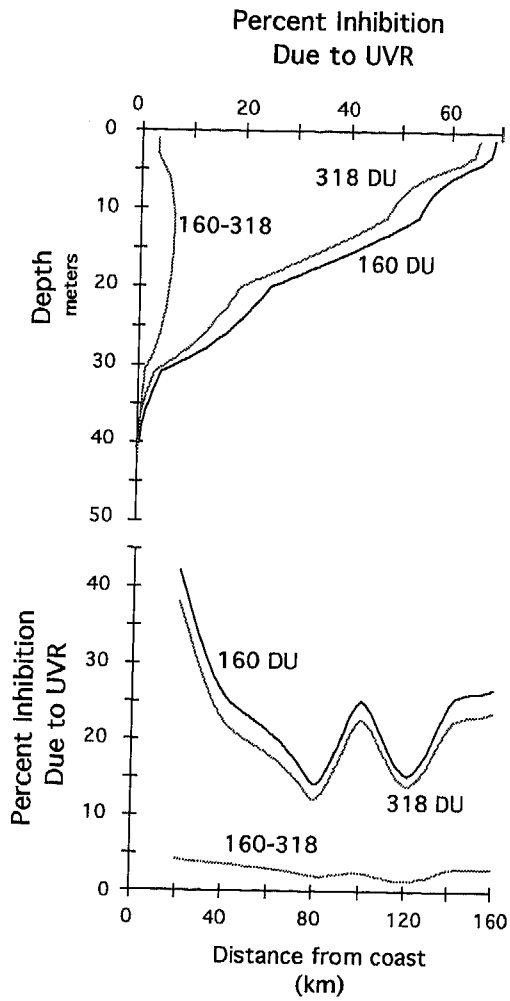

Figure 9. Depth profile of estimated percent inhibition of PAR-dependent rates of daily primary production within the diatom-dominated communities of Dallman Bay at station 700.040, when ambient O_3 concentrations are 318 DU or 160 DU. Bottom: Estimated percent inhibition of PAR-dependent rates of daily integrated primary production in the upper 100 m of different LTER 700 Line transect station, when ambient O_3 concentrations are 318 DU or 160 DU. The additional O_3-dependent UVB inhibition resulting from a drop in O_3 concentrations from 318 to 160 DU is shown by the 160–318 line in each panel.

over the day but field data analyses are not yet sufficient to incorporate nonlinear changes in BWF in the present calculations.

With knowledge of the *in situ* BWF for Antarctic diatom-dominated communities, the *in situ* spectral irradiance and the PAR-only rates of primary production, we estimated the UV-dependent rates of primary production for conditions when stratospheric O_3 was 318 DU (*i.e.* values for 14 November 1991) and for conditions when stratospheric O_3 might be reduced to 160 DU (Fig. 7). By our calculations, ambient UVR on 14 November 1991 could have decreased primary production in surface waters by up to 60%, forcing carbon uptake rates to subsurface maxima across the entire 700 transect Line. By enhanced UVB radiation to a level representative of a 50% reduction in stratospheric O_3 and symptomatic of exposures under the Antarctic O_3 hole, primary production was decreased in surface and subsurface waters by up to 16% and resulted in further deepening of the subsurface maxima in carbon fixation.

The magnitude of the UVR inhibition effects was estimated to vary with time and depth (Fig. 7). Daily integrated UVR inhibition effects decreased with depth and could not be detected at depths below *ca* 36 m (Fig. 8). Water column integrated loss of primary production due to UVR at the time of measurement averaged *ca* 25% (Fig. 9), with greatest loss of absolute fixed carbon occurring in the diatom-dominated communities in Dallmann Bay. Water column integrated inhibition declined *ca* 5% following a decrease in stratospheric O_3 concentration from 360 to 160 DU. The magnitude of the additional O_3-dependent inhibition on the spectrally modeled rates of UV-dependent primary production is nonlinearly related to stratospheric O_3 concentration (18) and the percent inhibition by enhanced UVB radiation are pre-

dicted to increase exponentially as the O_3 depletion becomes more severe.

CONCLUSIONS

Our spectral modeling effort demonstrates how a field-derived *in situ* BWF for carbon fixation could be used to estimate the impact of UVR on primary production in a limited region of Southern Ocean coastal waters. For the first time, care was taken to incorporate the diurnal variation of UVR fluence rate and vertical attenuation of the water to estimate UVR damages. Results show that considerable overestimation of primary production can be made using classical primary production measurements if *in situ* incubation and photosynthetron measurements in the absence of UVR tend to release the cells from UVR inhibition. It is also demonstrated that BWF differ between field and laboratory measurements and that accurate field measurements of UVR effects on primary production will require careful consideration of the algorithms used, as well as the time and space scales over which such UVR spectral models might be presently applied to predict ecosystem responses to changing UV climatology. For our study site, ambient UVR was a major parameter influencing the vertical distribution of primary production in the coastal waters of the Southern Ocean in the spring of 1991. In comparison to full spectral UVR effects, the short-term effect of the O_3 diminution in the present study was small but measurable. Results would have differed had different climatological, hydrographic and/or phytoplankton, with differing UVR sensitivities, been present.

Acknowledgements—We thank R. C. Smith for making the LTER 700 Line PAR data and the six *Icecolors '90* UVR-PAR spectral light profiles available for the present study. We also thank S. Madronich for providing patient training and generous use in his UVR-PAR code and C. R. Booth for providing the Palmer Station UVR-PAR data sets since 1991. H. A. Matlick and M. Moline provided valuable technical assistance and T. J. Evens, B. Kroon, R. Jovine, M. Moline, O. Schofield and the women and men of Palmer Station and the RV *Polar Duke* provided much assistance in the collection of the primary production data. Drs. S. Madronich and M. Moline provided much valued discussion and encouragement during the preparation of the manuscript. Research funding was provided by National Science Foundation grants DPP90-901127 and DPP-92-20962 awarded to B.B.P. This is a joint Icecolors'93 and LTER (LTER #95) publication.

REFERENCES

1. Smith, R. C., R. R. Bidigare, B. B. Prézelin, K. S. Baker and J. M. Brooks (1987) Optical characterization of primary productivity across a coastal front. *Mar. Biol.* **96**, 575–579.
2. Platt, T. and S. Sathyendranath (1988) Oceanic primary production: estimation by remote sensing at local and regional scales. *Science* **241**, 1613–1620.
3. Balch, W. M., M. R. Abbott and R. W. Eppley (1989) Remote sensing of primary production. I. A comparison of empirical and semi-analytical algorithms. *Deep-Sea Res.* **36**, 281–295.
4. Platt, T., S. Sathyendranath and P. Ravindran (1990) Primary production by phytoplankton: analytical solutions for daily rates per unit area of water surface. *Proc. R. Soc. Lond. B* **241**, 101–110.
5. Longhurst, A., S. Sathyendranath, T. Platt and C. Caverhill (1995) An estimate of global primary production in the ocean from satellite radiometer data. *J. Plankton Res.* **17**, 1245–1271.
6. Platt, T. (1986) Primary production of ocean water column as a function of surface light intensity: algorithms for remote sensing. *Deep-Sea Res.* **33**, 149–163.
7. Bidigare, R. R., B. B. Prézelin and R. C. Smith (1992) Bio-optical models and the problems of scaling. In *Primary Productivity and Biogeochemical Cycles in the Sea* (Edited by P. G. Falkowski and A. D. Woodhead), pp. 175–212. Plenum, New York.
8. Sathyendranath, S., T. Platt, C. Caverhill, R. E. Warnock and M. R. Lewis (1989) Remote sensing of oceanic primary production: computations using a spectral model. *Deep-Sea Res.* **36**, 431–453.
9. Morel, A. (1991) Light and marine photosynthesis: a spectral model with geochemical and climatological implications. *Prog. Oceanogr.* **26**, 263–306.
10. Davis, R. R., J. M. Napp, C. C. Moore and J. R. V. Zanaveld (1994) Long-term deployment of first-generation *in situ* spectral absorption meters and transmissionometers. *EOS Trans. Am. Geophys. Union* **75**(3), 22.
11. Lewis, M. R., R. E. Warnock and T. Platt (1985) Measuring photosynthetic action spectra of natural phytoplankton populations. *J. Phycol.* **21**, 310–315.
12. Schofield, O., R. R. Bidigare and B. B. Prézelin (1990) Spectral photosynthesis, quantum yield and blue-green light enhancement of productivity rates in the diatom *Chaetoceros gracile* and the prymnesiophyte *Emiliana huxleyi*. *Mar. Ecol. Prog. Ser.* **64**, 174–186.
13. Weiler, S. and P. Penhale (eds.) (1994) *Ultraviolet Radiation and Biological Research in Antarctica*, Vol. 62. American Geophysical Union, Washington, DC.
14. Madronich, S. (1993) UV radiation in the natural and the perturbed atmosphere. In *UV-B Radiation and Ozone Depletion* (Edited by M. Tevini), pp. 17–69. Lewis, Boca Raton, FL.
15. D. Albritton and R. Watson (eds.) (1995) *Scientific Assessment of Ozone Depletion*. World Meteorological Organization, Global Ozone Research and Monitoring Project, report no. 37.
16. Smith, R. C., B. B. Prézelin, K. S. Baker, R. R. Bidigare, N. P. Boucher, T. Coley, D. Karentz, S. MacIntyre, H. A. Matlick, D. Menzies, M. Ondrusek, Z. Wan and K. J. Waters (1992) Ozone depletion: ultraviolet radiation and phytoplankton biology in Antarctic waters. *Science* **255**, 952–959.
17. Smith, R. C. and K. S. Baker (1982) Assessment of the influence of enhanced UV-B on marine primary productivity. In *The Role of Solar Ultraviolet in Marine Ecosystems* (Edited by J. Calkins), pp. 509–537. Plenum, New York.
18. Boucher, N. P. and B. B. Prézelin (1996) An *in situ* biological weighting function for UV inhibition of phytoplankton carbon fixation in the Southern Ocean. *Mar. Ecol. Prog. Ser.* (In press)
19. Prézelin, B. B., S. Madronich, N. Boucher, and H. A. Matlick (1995) Springtime variability and predictive accuracy of *in situ* biological weighting functions for UV inhibition of primary production in Antarctic phytoplankton. *Limnol. Oceanogr.* Abstract supplement, p. 2.
20. Prézelin, B. B. and H. A. Matlick (1996) Diurnal and day-to-day variations in biological weighting functions quantifying the photoinhibition of Antarctic primary production by UV radiation. *EOS Trans. Am. Geophys. Union* **76**(3), 138.
21. Prézelin, B. B., M. Moline and H. A. Matlick (1996) UV effects on ice algae. In *Sea Ice Biology* (Edited by M. Lizotte and K. Arrigo). AGU Research Series. (In press)
22. Williamson, C. E. and H. E. Zagarese (eds.) (1994) Impact of UV-B radiation on pelagic freshwater ecosystems. *Arch. Hydrobiol.* **43**, 1–226.
23. Waters, K. and R. C. Smith (1991) Palmer LTER: a sampling grid for the Palmer LTER program. *Antarct. J. U.S.* **27**, 236–238.
24. Moline, M. A. and B. B. Prézelin (1996) High-resolution time-series data for primary production and related parameters at a Palmer LTER coastal site: implications for modeling carbon fixation in the Southern Ocean. *Polar Biol.* **14**. (In press)
25. Baker, K. and R. Frouin (1987) Relation between photosynthetically available radiation and total insolation at the ocean surface under clear skies. *Limnol. Oceanogr.* **32**, 1370–1377.
26. Prézelin, B. B., R. R. Bidigare, H. A. Matlick, M. Putt and B. Ver Hoven (1987) Diurnal patterns of size fractioned primary productivity across a coastal front. *Mar. Biol.* **4**, 563–574.
27. Parsons, T., Y. Maita and C. Lalli (1984) *A Manual of Chemical*

and Biological Methods for Sea Water Analysis. Pergamon, Oxford.
28. Neale, P. J. and P. J. Richerson (1987) Photoinhibition and the diurnal variation of phytoplankton photosynthesis. I. Development of a photosynthesis–irradiance model from studies of *in situ* responses. *J. Plankton Res.* **9**, 167–193.
29. Prézelin, B. B., N. P. Boucher and R. C. Smith (1994) Marine primary production under the influence of the Antarctic ozone hole: *Icecolors '90.* In *Ultraviolet Radiation and Biological Research in Antarctica,* Vol. 62 (Edited by S. Weiler and P. Penhale), pp. 159–186. American Geophysical Union, Washington, DC.
30. Booth, C. R., T. B. Lucas, J. H. Morrow, S. C. Weiler and P. A. Penhale (1994) The United States National Science Foundation's polar network for monitoring ultraviolet radiation. In *Ultraviolet Radiation and Biological Research in Antarctica,* Vol. 62 (Edited by S. Weiler and P. Penhale), pp. 17–37. American Geophysical Union, Washington, DC.
31. Rundel, R. D. (1983) Action spectra and estimation of biologically effective UV radiation. *Physiol. Plant.* **58**, 360–366.
32. Vernet, M., E. A. Brody, O. Holm-Hansen and B. G. Mitchell (1994) The response of Antarctic phytoplankton to ultraviolet radiation: absorption, photosynthesis, and taxonomic composition. In *Ultraviolet Radiation and Biological Research in Antarctica,* Vol. 62 (Edited by S. Weiler and P. Penhale), pp. 143–158. American Geophysical Union, Washington, DC.
33. Prézelin, B. B., N. P. Boucher and O. Schofield (1994) Evaluation of field studies of UV-B radiation effects on Antarctic marine primary productivity. In *Stratospheric Ozone Depletion and UV-B Radiation in the Biosphere,* Vol. 118 (Edited by H. Bigg and M. E. B. Joyner), pp. 181–194. NATO Advance Study Institute Series.
34. United Nations Environment Programme, UNEP (1994) Environmental Effects of Ozone Depletion—1994 Update. *AMBIO* **24**, 137–196.
35. Scientific Committee on Protection of the Environment, SCOPE (1993) Effects of increased ultraviolet radiation on global ecosystems. Scientific Committee on Problems of the Environment, 51 bd de Montmorency, 75016 Paris, France.
36. International Arctic Science Committee, IASC (1995) Effects of increased ultraviolet radiation in the Arctic. International Arctic Science Committee (IASC) Report 2, Oslo, Norway.
37. Molina, L. T. and M. J. Molina (1986) Absolute absorption cross sections of ozone in the 185- to 350-wavelength range. *J. Geophys. Res.* **91**, 14,501–14,508.
38. Quesada, A., J.-L. Mouget and W. F. Vincent (1995) Growth of Antarctic cyanobacteria under ultraviolet radiation: UVA counteracts UVB inhibition. *J. Phycol.* **31**, 242–248.
39. Steeman-Nielsen, E. (1964) On a complication in marine productivity work due to the influence of ultraviolet light. *J. Cons. Int. Exp. Mer* **29**, 130–135.
40. Jerlov, N. (1950) Ultraviolet radiation in the sea. *Nature* **166**, 111.
41. Lorensen, C. J. (1979) Ultraviolet radiation and phytoplankton photosynthesis. *Limnol. Oceanogr.* **24**, 1117–1120.
42. Kirk, J. T. O. (1994) Optics of UV-B radiation in natural waters. In *Advances in Limnology: Impact of UV-B Radiation on Pelagic Ecosystems* (Edited by C. E. Williamson and H. E. Zagarese), pp. 1–16. *Archiv für Hydrobiologie,* Stuttgart.
43. Scully, N. M. and D. R. S. Lean (1994) The attenuation of ultraviolet radiation in temperate lakes. In *Advances in Limnology: Impact of UV-B Radiation on Pelagic Ecosystems* (Edited by C. E. Williamson and H. E. Zagarese), pp. 135–144. *Archiv für Hydrobiologie,* Stuttgart.
44. Vincent, W. F. and S. Roy (1993) Solar UV-B and aquatic primary production: damage, protection and recovery. *Environ. Rev.* **1**, 1–12.
45. Caldwell, M. M., L. B. Camp, C. W. Warner and S. D. Flint (1986) Action spectra and their key role in assessing biological consequences of solar UV-B radiation change. In *Stratospheric Ozone Reduction, Solar Ultraviolet Radiation and Plant Life* (Edited by R. C. Worrest and M. M. Caldwell), pp. 87–111. NATO ASI series, G8, Springer-Verlag, Berlin.
46. Coohill, T. P. (1994) Exposure response curves, action spectra and amplification factors. In *Stratospheric Ozone Depletion and UV-B Radiation in the Biosphere,* Vol. 118 (Edited by H. Bigg and M. E. B. Joyner), pp. 57–62. NATO Advance Study Institute Series.
47. Arrigo, K. R. (1994) Impact of ozone depletion on phytoplankton growth in the Southern Ocean: large-scale spatial and temporal variability. *Mar. Ecol. Prog. Ser.* **114**, 1–12.
48. Cullen, J. J., P. J. Neale and M. P. Lesser (1992) Biological weighting function for the inhibition of phytoplankton photosynthesis by ultraviolet radiation. *Science* **258**, 646–650.
49. Madronich, S., R. L. McKenzie, M. M. Caldwell and L. O. Bjorn (1995) Changes in ultraviolet radiation reaching the earth's surface. *AMBIO* **24**, 143–152.
50. Smith, R. C., K. S. Baker, K. K. Hwang, D. Menzies and K. J. Waters (1992) Palmer LTER program: hydrography and optics within the peninsula grid, November 1991 cruise. *Antarct. J. U.S.* **27**, 250–252.
51. Smith, W. O. and D. M. Nelson (1985) Phytoplankton bloom produced by a receding ice edge in the Ross Sea: spatial coherence with the density field. *Science* **277**, 163–166.
52. Prézelin, B. B., N. P. Boucher, M. A. Moline, E. Stephens, K. Seydel and K. Scheppe (1992) Palmer LTER program: spatial variability in phytoplankton and surface photosynthetic potential within the Peninsula grid, November 1991. *Antarct. J. U.S.* **27**, 242–245.
53. Moline, M. A., B. B. Prézelin, O. Schofield and R. C. Smith (1996) Temporal dynamics of coastal Antarctic phytoplankton: environmental driving forces through a 1991–1992 summer diatom bloom on the nutrient and light regime. In *Antarctic Communities* (Edited by B. Battaglia, J. Valencia and D. W. H. Walton) Cambridge Press. (In press)
54. Falkowski, P. G. and A. D. Woodhead (eds.) (1992) *Primary Productivity and Biogeochemical Cycles in the Sea.* Plenum Press, New York.
55. Smith, R. C., B. B. Prézelin, R. R. Bidigare and K. S. Baker (1989) Bio-optical modeling of photosynthetic production in coastal waters. *Limnol. Oceanogr.* **34**, 1524–1544.
56. Schofield, O., B. M. A. Kroon and B. B. Prézelin (1995) Impact of ultraviolet-B radiation on photosystem II activity and its relationship to the inhibition of carbon fixation rates for Antarctic ice algae communities. *J. Phycol.* **31**, 703–715.
57. Boucher, N. P. (1994) Antarctic phytoplankton primary production under enhanced flux of ultraviolet radiation: a bio-optical approach. PhD Thesis, University of California at Santa Barbara.